

Reduced L_1 level width and Coster-Kronig yields by relaxation and continuum interactions in atomic zinc

S. Fritzsche, B. Fricke, and W.-D. Sepp

Fachbereich Physik, Universität Kassel, D-3500 Kassel, Germany

(Received 23 September 1991)

Calculations of the level width $\Gamma(L_1)$ and the f_{12} and f_{13} Coster-Kronig yields for atomic zinc have been performed with Dirac-Fock wave functions. For $\Gamma(L_1)$, a large deviation between theory and evaluated data exists. We include the incomplete orthogonality of the electron orbitals as well as the inter-channel interaction of the decaying states. Orbital relaxation reduces the total rates in all groups of the electron-emission spectrum by about 10–20%. Different, however, is the effect of the continuum interaction. The L_1 - $L_{23}X$ Coster-Kronig part of the spectrum is definitely reduced in its intensity, whereas the MM and MN spectra are slightly enhanced. This results in a reduction of Coster-Kronig yields, where for medium and heavy elements considerable discrepancies have been found in comparison to relativistic theory. Briefly, we discuss the consequences of our calculations for heavier elements.

PACS number(s): 31.20.Di, 32.80.Hd, 32.70.Fw

I. INTRODUCTION

The level width of a vacant state is the sum of all partial widths for the radiative Γ_R , Auger Γ_A , as well as Coster-Kronig (CK) decay Γ_{CK} . Usually, many different decay channels, varying in their individual transition rates, occur. If Coster-Kronig transitions are allowed, they govern the lifetimes of atomic inner-shell vacancies and the radiative and Auger decay will then be less important. In this context Auger transitions are defined as radiationless transitions between shells with different principal quantum numbers, whereas in CK transitions the vacancy is shifted within the same (major) shell.

Total transition rates for inner-shell vacancies can often be calculated appropriately in the independent-particle model. This was confirmed for K -shell level widths [1–3] and usually also applies to the various K -shell decay spectra [4]. A similar agreement for the L -shell widths $\Gamma(L_2)$ and $\Gamma(L_3)$ over the whole atomic range was obtained with Dirac-Hartree-Slater (DHS) wave functions [5]. These calculations demonstrated that the total widths are merely slightly sensitive to the employed coupling scheme and electron correlation. Surprisingly, however, even relativistic calculations failed for the theoretical prediction of the L_1 level widths $\Gamma(L_1)$ in medium- Z elements ($19 \leq Z \leq 48$). For example, the DHS computations by Chen, Crasemann, and Mark [5] overestimated the total width in atomic zinc by a factor of 3. Their theoretical value of about 9.6 eV has to be compared with the evaluated semiempirical one [6] of 3.28 eV and deviations like this occur in the range reported. Similar results were also obtained in other approximate Hartree-Slater calculations [7]. Therefore, the need for a more accurate many-body calculation of the low-energy CK transitions became evident.

Chen and co-workers [5] calculated the Auger transition rates from perturbation theory using frozen orbitals. If the configuration interaction (CI) and the fine-structure

splitting in the final states are neglected, as it is usually assumed in single-configuration calculations, the description of the many-electron system may then be reduced to a two-hole picture. However, it is now known that individual transition rates may deviate significantly from one another (up to a factor of 10 or even more) [8]. This underlines the role of an appropriate coupling scheme in the computations.

Recently, measurements for the Coster-Kronig yields in some medium- Z and heavier elements have been reported [9–12]. The yield f_{ij} describes the probability for promoting the vacancy from subshell L_i to subshell L_j . The CK probability in ${}_{39}\text{Y}$ and ${}_{47}\text{Ag}$ were measured by differential photoionization of the subshells using synchrotron radiation. In ${}_{39}\text{Y}$, Jitschin, Grosse, and Röhl [9] found a ratio $f_{13} = 0.49 \pm 0.09$ which is remarkably smaller than the theoretical prediction of 0.747 reported by Chen, Crasemann, and Mark [5]. The same theoretical work overestimated the CK yield in silver [10], where f_{12} and f_{13} were found to be smaller by 35% and 18%, respectively. A similar trend of reduction, but of slightly better agreement with relativistic calculations, was found for various f_{23} yields [11,12].

One point that was neglected in all earlier calculations is the orbital relaxation when going from the initial to the final states. The effect of the nonorthogonality on autoionization rates has been investigated at first nonrelativistically for the neon K - LL spectrum [13]. We confirmed these results with our relativistic code as a test case. Further significant changes in the transition rates by relaxation were also reported in the Ar L_1 - $L_{23}M$ Coster-Kronig spectra [14] as well as in the near-threshold region of photoionization cross sections [15].

Here, we report on multiconfiguration Dirac-Fock (MCDF) calculations for the complete nonradiative decay spectrum of the L_1 hole state in ${}_{30}\text{Zn}$ corrected for relaxation as well as continuum interactions of the decaying states. We chose atomic zinc for our investigations

because there a large deviation for the L_1 total width was found. Furthermore, free zinc atoms possess closed shells and therefore only relatively few decay channels. In heavier open-shell systems the number of energetically allowed channels quickly becomes prohibitively large, which further results in a practical limitation.

A brief review of the theoretical formulation is given in the next section. Then we present and discuss our results and compare them with Krause's semiempirical data [6,16]. To include the relaxation corrections in the total widths a suitable procedure has to be chosen. This and its possible extension to more complex (open-shell) atoms will be discussed.

II. BRIEF REVIEW OF THEORY

Considering the Auger decay within a two-step model the transition rates are usually derived from first-order perturbation theory. To include additional configuration interactions between an (isolated) quasidecrete initial state and the various autoionization continua, the theoretical description was improved by Aberg and Howat [13,17]. Supplementary to Fermi's rule a principal-value integration P along the free-electron energy of all the various continua has to be performed to obtain the partial radiationless rate for a transition from the initial hole state ψ_i to the final ionized state $\psi_{\alpha\epsilon}$ [17,18]

$$T_{\alpha i} = 2\pi \left| \langle \psi_{\alpha\epsilon} | H - E | \psi_i \rangle + P \sum_{\beta=1}^N \int_0^{\infty} \frac{V_{\alpha\beta}(\epsilon, \tau, E) \langle \psi_{\beta\tau} | H - E | \psi_i \rangle}{E - E_{\beta} - \tau} d\tau \right|^2. \quad (1)$$

Here, ϵ and τ are the kinetic energies of the outgoing electron and the electron in an intermediate state, respectively, and β goes over all the various continua (distinguished by their symmetry), which involve in their energy range the total initial hole-state energy E . Further, $V_{\alpha\beta}$ denotes the interaction matrix in lowest order between different continuum states

$$\langle \psi_{\alpha\epsilon} | H - E | \psi_{\beta\tau} \rangle = V_{\alpha\beta}(\epsilon, \tau, E) + \delta_{\alpha\beta} \delta(\epsilon - \tau) (\tau + E_{\beta} - E). \quad (2)$$

This indicates that the Hamiltonian matrix need not be diagonalized first with respect to the chosen continuum basis set $\{\psi_{\beta\tau}\}$. An additional negligible (imaginary) contribution to the transition amplitude is omitted from Eq. (1).

Besides the coupling of the continua, this scattering formulation also includes the correct *incoming-wave* boundary conditions required for all ionization processes.

To calculate these modified transition rates we used wave functions at the MCDF level [19]. Here intermediate coupling is included by configuration interaction (CI) and diagonalizing the Hamiltonian submatrices for bound states of the same symmetry.

The configuration-interaction theory of a quasidecrete state embedded in the continuum was originally formulated by Fano [20]. Due to the CI with the various con-

tinua the resonance energy E differs slightly from the stationary energy E_i obtained by a variational calculation. This resonances energy arises from the diagonalization of the total Hamiltonian (sub)matrix, including the various continua. The computation of the shift $\Delta = E - E_i$ requires, once more, principal-value integrations similar to Eq. (1) (now replacing $V_{\alpha\beta}$ by $\langle \psi_i | H - E | \psi_{\beta\tau} \rangle$). Usually, this energy shift lowers the transition energy ($\Delta < 0$) and may be of particular importance in the case of strong Auger and Coster-Kronig transitions [21,22]. This point will be discussed further in the next section.

Our relativistic Auger program, using an intermediate coupling scheme, extends Grant's atomic-structure code [19] to radiationless transitions. Due to the decay of the initial state by the emission of an electron we start with different calculations belonging to the initial hole and final double-hole states. Then, the transition energies of the free electrons may be derived by simply taking the differences of the total energies (possibly involving the shift Δ).

One of the difficulties with accurate Auger-rate calculations is the appropriate generation of the free-electron waves which couple to the final $(N-1)$ -electron state to conserve the total angular momentum and the parity of ψ_i . To obtain these continuum spinors we solve the (complete) DF equations in the static potential of the considered final state. Orthogonality with respect to the bound-electron orbitals of the final states is enforced by Lagrange multipliers. In frozen-orbital computations orthogonality with respect to the initial-state orbitals was obtained by a Schmidt-orthogonalization procedure. We will show the effects of these additional somewhat *arbitrary* exchange terms in the DF equations in connection with our results.

In the MCDF model each transition matrix element [for instance the first term in Eq. (1)] is expanded in a sum of matrix elements between configuration state functions (CSF's) belong to the initial and final states. The final-state CSF's contain a continuum orbital for the outgoing electron. It should be kept in mind, however, that owing to the different permitted angular momentum and parity quantum numbers of the free-electron wave the double-hole state of the remaining ion may contribute to different transitions. Therefore, we will use the term *decay channel* for the total N -electron final state to distinguish it from the residual ionic state.

In the frozen-orbital approximation the transition operator $(H - E)$, incorporating the full Hamiltonian, is reduced to the two-electron interaction. Neglecting the principal-value terms in Eq. (1) this type of calculation corresponds to Wentzel's ansatz [23]. For the electron repulsion in the Hamiltonian we mostly used the instantaneous Coulomb repulsion, but computations with the additional transverse Breit interaction show that, in the transition operator, relativistic effects play only a minor role in our test case atomic zinc (cf. column *B* in Fig. 1).

The evaluation of the matrix elements with frozen orbitals (*unrelaxed* transition rates) may be performed easily by employing the decomposition in angular coefficients and radial integrals [19,24]. However, the (more-realistic) electron relaxation results in nonorthogonal-

orbital sets of the separate optimized initial and final states. This means that, for the calculation of the matrix elements, all the overlap factors (or at least the strongest ones) have to be involved. In particular, the one-electron operators in the Hamiltonian and the total energy $E \approx E_i$ now contribute to the transition amplitudes.

Therefore, to calculate also relaxed transition rates, we expanded the separately optimized CSF's in Slater determinants and used the known expressions of Löwdin [18,25] for each pair of (nonorthogonal) determinants to compute the complete matrix elements. Obviously, owing to the large numbers of overlap integrals, this type of calculation is very time consuming.

For the (complete) expansion of the CSF's in determinants, a computer-program module was developed. For a variety of one- and two-body operators it facilitates the computation of matrix elements between CSF's with incomplete orthogonality. For reasons of economy, how-

ever, in these *relaxed* transition rates we calculated the additional correction terms (i.e., the large number of the matrix elements in the principal-value integrant) in the frozen-orbital approach.

Here, the features of our program have only been presented in a brief outline. More computational details, in particular concerning nonorthogonal orbital sets in the initial and final states, will be given elsewhere. The method employed for the principal-value integration was described recently [26].

III. RESULTS AND DISCUSSION

A. Energy shifts

Because of their low energy and large wave-function overlap, CK transitions are usually very intensive. Thus, they can shorten the lifetimes of free atoms considerably if they are allowed. In our MCDF calculations of atomic zinc we obtained the results that the two lines of the $L_1-L_3M_1$ spectrum with angular momenta $J=1$ and 2 in the final ionic state have transition energies of about 4.7 and 6.5 eV, respectively. Especially, the Coster-Kronig decay to the $J=1$ final state contributes strongly to the total width with about 0.8 eV (in the frozen-orbital approach). The super Coster-Kronig and the $L_1-L_2M_1$ transitions, on the other hand, are all forbidden energetically, whereas the onset of the other CK parts of the spectrum at about 12 eV is not so crucial with respect to a small energy shift.

Owing to these low energies of the $L_1-L_3M_1$ spectrum, it is necessary to investigate primarily the coupling of the quasisdiscrete initial $2s$ -vacancy state with the radiationless continua. This coupling is not involved in the multiconfiguration Dirac-Fock model but may lower its total energy in various cases. To calculate the resulting energy shift we include all the final continua belonging to the two-hole configurations of the $L_{23}X$ Coster-Kronig as well as the majority of the MM spectra. This selection of the final states, which is limited by practical reasons, will be further explained below in the context of the continuum interaction of the decaying states. But it ensures that the continua contributing most to the radiationless decay are included.

In MCDF calculations only the CI with other bound configurations may be considered. As atomic zinc has a closed-shell structure we chose a single-configuration calculation for the initial $2s$ -vacancy state. No significant energy shift should arise from the interaction with other bound configuration states.

From the study of binding energies [22] it is known that the level energy shift produced by Coster-Kronig fluctuations is particularly essential for many $2s$ -vacancy states. This was established by Chen's recent DHS computations [21] using Fano's theory [20]. He reports for ^{30}Zn an energy shift of -3.3 eV. We recalculate this shift, arising from the interaction with the radiationless continua, in the intermediate coupling scheme. For the final states with correct DF continuum waves and those spinors excluding the exchange terms in the DF equations of the free electrons, we found an energy shift of

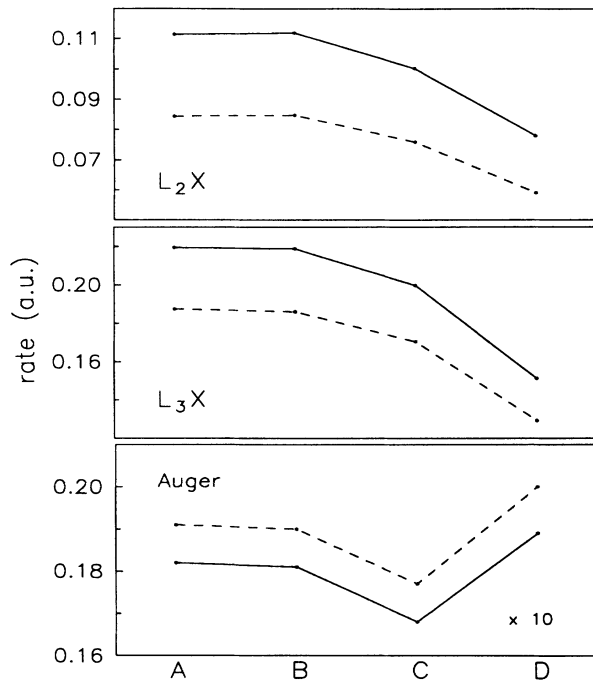


FIG. 1. Comparison of various theoretical approaches for the nonradiative partial widths of the L_1 shell. The sections of this figure correspond to the chosen decay spectra in Table I but in the bottom one (Auger) we have combined all the permitted decay channels from the MM and MN spectra. Simple frozen-orbital MCDF calculations with only the static Coulomb interaction in the transitions matrix elements (A) are shown together with analogous computations including also the relativistic (transverse) Breit interaction in the transition operator (B). Next (C) we present relaxed widths taking into account the complete nonorthogonality of the electron orbitals in the initial and final states. Finally, under D, these results are corrected for the continuum interaction as given by Eq. (1). Besides these calculations, solving the complete DF equations for the free-electron waves (solid line), we show approximate results (dashed line), neglecting the exchange interactions in the inhomogeneous DF equations for the emitted electrons. For details see the text. In the bottom part of this figure all values are multiplied by a factor of 10.

−2.9 and −3.1 eV, respectively. In these calculations we employed the orthonormal set of the initial-state orbitals also for the final states and, to keep it simple, we used only the Coulomb part of the two-electron interaction in the principal-value integration. This reduction in the total energy of the initial state lowers the L_1 - L_3M_1 spectra to about 1.8 eV ($J=1$) and 3.6 eV ($J=2$). One should have in mind, however, that for the doubly excited (final) two-hole states the fine-structure splitting in MCDF calculations is not very accurate. Therefore, a clear decision on whether these transitions would contribute to the $2s$ -vacancy decay is not possible. On the other CK and Auger spectra this energy shift of the initial state of about 3 eV is less important and we found only a negligible influence on their partial widths.

B. L_1 level width

To determine the total width and CK yields, the probabilities of all decay channels have to be calculated consecutively. Even for medium- Z elements this necessitates a large number of calculations. Atomic zinc has the advantage here that the $2s$ -vacancy state is well described by a single configuration.

The large number of CSF's for the final states is due to the coupling of the two holes. They may be divided by their stronger configuration mixing (but somewhat arbitrarily) into the four decay spectra shown in Table I. This table includes all considered configurations and the number of final double-hole states in ${}_{30}\text{Zn}$. Additionally, the decay channels are represented where continuum waves with different allowed angular momenta have been coupled to the final ionic state to conserve the total angular momentum J_i and the parity P_i of the initial state.

Extended average-level (EAL) calculations [19] were performed separately for the specified spectra. In such an EAL calculation the orbital wave functions are obtained by minimizing the statistically averaged energy of all levels included. Within each of these spectra the energy splitting is not too large, thus taking appropriately into account electron correlation by the limited configuration interaction in this range of intermediate coupling.

Following the improved theoretical description step by step we calculated the individual transition rates in various approaches. In Fig. 1 we compare the simple MCDF results in intermediate coupling with those corrected for electron relaxation and interchannel interactions of the decay channels for the different line groups. In columns A and B we present the results of frozen-orbital calculations where the initial-state orbitals were used also for the final states. The full Hamiltonian in the matrix elements is then reduced to the two-electron interaction. The results from a computation with the static Coulomb interaction (column A), compared with those including the additional Breit terms (column B), show that relativistic effects in the transition operator play only a minor role and may be neglected by more advanced computations.

The incomplete orthogonality of the orbital sets in the transition matrix elements is taken into account in column C . Orbital relaxation reduces the overall partial transition width within each of the chosen spectra. In the Auger spectra the decrease of about 10% is smaller than that for the CK decay of up to 20%. It should be mentioned, however, that relaxation does not lower equally all the individual rates included in these spectra.

Such *relaxed* transition-rate calculations require a large amount of CPU time. Because the individual transitions contribute very differently to the total widths we used an approximation procedure for the large number of individual Auger transitions whereas the full nonorthogonality was involved for the intense L_2X and L_3X CK spectra. The weaker Auger lines were sorted by their intensities. From the 46 allowed transitions (the sum of the MM as well as the combined MN and NN spectra), the 20 most intensive transitions cover about 98% of the unrelaxed Auger width. Only for these transitions was the complete electron relaxation taken into account in column C of Fig. 1. We note that this procedure would be particularly convenient for open-shell systems. Here, the number of decay channels increases dramatically, but the main contributions come from a few individual lines only.

In column D (Fig. 1) we give the results if both the relaxation and the interchannel coupling are included. Equation (1) shows that the interchannel interaction gives

TABLE I. Final hole-state configurations following the decay of a $2s$ vacancy in atomic zinc. From these configurations the number of all final states (divided somewhat arbitrarily into four decay spectra and listed here without their magnetic degeneracy) may be derived within the relativistic jj -coupling scheme. Of course, these numbers of final states are independent of the coupling scheme. Enhanced numbers of decay channels result from the coupling of different free-electron spinors to the final ionic states in a way which conserves the angular momentum and parity of the total system.

	Number of final two-hole states	Number of decay channels	Final hole-state configurations
L_2X	11	20	$2p_{1/2}3p, 2p_{1/2}3d, 2p_{1/2}4s$
L_3X^a	17	32	$2p_{3/2}3s, 2p_{3/2}3p, 2p_{3/2}3d$ $2p_{3/2}4s$
MM	35	63	$3s^2, 3s3p, 3s3d, 3p^2$ $3p3d, 3d^2$
MN, NN	11	19	$3s4s, 3p4s, 3d4s, 4s^2$

^aIf the L_1 - L_3M_1 transitions are not energetically possible, the number of final ionic states is reduced to 15 and only 28 Coster-Kronig decay channels occur in the L_3X spectrum.

a separate correction term to the transition amplitude. Difficulties arise here from the fact that all (significant) decay channels will interact with each other. Some simplification may be obtained by neglecting weak transitions. This is permissible as the interaction is closely connected to the decay strength of the channels. However, there is no proportionality and it is advisable not to omit weaker transitions in advance. We therefore performed a further EAL calculation with 62 CSF's including all CK and the majority of the Auger final states. Because of practical limitations we had to exclude some weak final states from the MM and MN spectra with individual relative transition probabilities $< 1\%$ of the total width.

With the double-hole wave functions of this large CSF expansion and all the derived continua we calculate the additional terms for each transition amplitude. Pronounced cancellation of the amplitudes may occur, resulting in a reduction of the individual rate. A remarkable reduction of the partial widths arises from this interaction for the L_2X and L_3X Coster-Kronig spectra. The partial Auger widths, on the other hand, will be enhanced due to this interchannel coupling. This means that a part of the CK intensity is shifted to the higher-energy transitions, but this does not explain the breakdown of the Coster-Kronig decay. The earlier conclusion [13] that continuum interactions mainly redistribute individual transition rates must therefore be modified. For the decay of a $2s$ vacancy the interchannel coupling results in a clear reduction of the total rate.

Parallel to the discussed approaches (compare the solid line), Fig. 1 shows a further reduction of the partial width if the exchange of the emitted electron with the stationary bound electrons is neglected (dashed line). To save a further equally large amount of CPU time we give only a crude approximation for relaxation and interchan-

nel interactions by changing the solid curve by the same factor as derived from the simple frozen-orbital MCDF results (A). This illustrates the influence of exchange, noting, however, that in low-energy transitions a considerable contribution to the nonlocal exchange terms in the DF equations may arise from the Lagrange multipliers, which must be included to force orthogonality for the continuum spinors.

In Table II we compare our results with theory [5] and evaluated data [6,16]. As pointed out above, pure-DF calculations are largely independent of the coupling scheme and therefore our results (I) are very similar to the DHS calculations of Chen, Crasemann, and Mark [5]. In their computations they obtained the exchange by the local-potential Slater approximation. The improved values (II) are corrected for electron relaxation as well as the intercontinuum coupling. In addition, we have listed the various widths and CK yields (III), valid if it is assumed that the $L_1-L_3M_1$ decay is not permitted energetically, and listed the reduced values neglecting the exchange for the continuum orbitals (IV). In these two approaches the total widths will be reduced by 10% and 25%, respectively, and show better agreement with the calculated data of Krause [6,16].

C. Coster-Kronig yields

We consider the shifts of the CK yields here if we go beyond a simple MCDF calculation with orthogonal orbitals. Even though the continuum interaction enforces the reduction of the CK transition strength, it does not shift the f_{12} and f_{13} ratio appreciably. This obviously occurs because in zinc almost all of the $2s$ vacancies are promoted via Coster-Kronig decay. Therefore, a clearer impression is obtained if we consider the relative effects

TABLE II. Transition rates, level widths,^a and Coster-Kronig yields of the L_1 decay spectra in $_{30}\text{Zn}$.

	Total transition rates (ma.u) ^b			Level widths (eV) $\Gamma(L_1)$	Coster-Kronig yields	
	L_2X	L_3X	Auger		f_{12}	f_{13}
Evaluation ^c				3.28	0.29	0.54
Theory ^d	100.2	234.9	17.53	9.60	0.284	0.666
Present work (I) ^e	111.4	219.4	18.03	9.49	0.319	0.629
Present work (II) ^f	78.0	151.3	18.83	6.75	0.314	0.610
Present work (III) ^g	78.0	128.2	18.83	6.12	0.347	0.570
Present work (IV) ^h	59.1	108.7	19.94	5.11	0.315	0.579

^aThe radiative partial width was estimated by Scofield [27] to be $\Gamma_r \approx 0.006$ eV and may therefore be neglected by the considerations.

^b1 ma.u = 0.02721 eV/ \hbar = 4.134×10^{13} s⁻¹.

^cReferences [6,16].

^dReference [5].

^eMulticonfiguration Dirac-Fock calculations. The continuum orbitals were generated in the (stationary) mean field of the bound electrons by solving the complete DF equations.

^fRelaxed-orbital MCDF results corrected for interchannel coupling.

^gSame calculations as in (II) but without the $L_1-L_3M_1$ decay rates. See text for details.

^hMCDF calculations neglecting the exchange terms for the continuum orbitals. The continuum spinors were generated in the (stationary) mean field of the bound electrons. Then the values were corrected for relaxation and channel coupling by taking the same ratios as in the simple frozen-orbital results.

on the Auger channels, whose yield is enlarged by about 50%. This increase of the Auger part arises almost completely from the continuum interaction whereas the relaxation of the electrons lowers the total rates in each of the different spectra.

This is worth mentioning since significant discrepancies in comparison to theory were found for the CK yields in heavy atoms. In high- Z systems the Auger yields as well as radiative decay increase, and consequently the CK yields will decrease. For instance, the summed CK part $f_{12} + f_{13}$ of a $2s$ vacancy amounts to 80% in $_{47}\text{Ag}$ and to about 50% for the rare-earth elements [5]. Thus, similar changes in the transitions rates, if taking into account the dynamic and relaxation effects, would result in a remarkable reduction of the CK yields in heavier elements.

For these heavier elements this could bring the theory into better agreement with experiment. To date, however, it is beyond our computer facilities to explore such complex systems as $_{39}\text{Y}$ or $_{47}\text{Ag}$ for which measurements have been performed recently [9,10]. In these open-shell atoms, both the number of overlapping orbitals as well as the decay channels enlarged drastically. However, we will try to improve our code to make it more manageable and faster in the future. At least our suggested procedure, applying the complete relaxation only to the most striking transitions, seems to be appropriate in such computations.

IV. CONCLUSIONS

The L_1 level width and Coster-Kronig yields in free zinc atoms have been calculated. These hole-state prop-

erties were evaluated earlier [6,16]. Large deviations of theoretical results stimulated a reinvestigation which took into account relaxation as well as dynamic corrections from scattering theory.

In comparison to the independent-particle model a better agreement was achieved but a discrepancy remains for the total widths, which demonstrates that further electron correlations not only redistribute individual rates but also alter the total probabilities. Now, the L_1 width is within a factor of about 2 of the evaluated value.

Whereas the orbital relaxation results in an overall reduction of the transition rate, the continuum interaction clearly changes the proportion of the L_1 Auger and CK probabilities. As a consequence the f_{12} and f_{13} Coster-Kronig yields are reduced. This tendency agrees with recent measurements in the heavier atoms, for instance $_{47}\text{Ag}$. To date, the analogous calculations as described above for such open-shell systems require exhaustive computer facilities. However, a theoretical description in the intermediate coupling scheme is needed because these computations have shown that due to many-body effects (even total) transition rates are strongly state specific to the initial and final states. This applies to both the electron relaxation and, more pronounced, the scattering approximation.

ACKNOWLEDGMENTS

This work was supported by the Gesellschaft für Schwerionenforschung (GSI) and Deutsche Forschungsgemeinschaft (DFG).

-
- [1] E. J. McGuire, Phys. Rev. A **2**, 273 (1970).
 - [2] D. L. Walters and C. F. Bhalla, Phys. Rev. A **3**, 1919 (1971).
 - [3] M. H. Chen, B. Crasemann, and H. Mark, Phys. Rev. A **21**, 436 (1980).
 - [4] W. N. Asaad and D. Petrini, Proc. R. Soc. London, Ser. A **350**, 381 (1976).
 - [5] M. H. Chen, B. Crasemann, and H. Mark, Phys. Rev. A **24**, 177 (1981).
 - [6] M. O. Krause and J. H. Oliver, J. Phys. Chem. Ref. Data **8**, 329 (1979).
 - [7] E. J. McGuire, Phys. Rev. A **3**, 587 (1971).
 - [8] M. H. Chen, Phys. Rev. A **40**, 2365 (1989); M. H. Chen and B. Crasemann, *ibid.* **40**, 4330 (1989).
 - [9] W. Jitschin, G. Grosse, and P. Röhl, Phys. Rev. A **39**, 103 (1989).
 - [10] S. L. Sorensen, R. Carr, S. J. Schaphorst, S. B. Whitfield, and B. Crasemann, Phys. Rev. A **39**, 6241 (1989).
 - [11] J. L. Campbell, P. L. McGhee, R. R. Gingerich, R. W. Ollerhead, and J. A. Maxwell, Phys. Rev. A **30**, 161 (1984).
 - [12] A. L. Catz, Phys. Rev. A **36**, 3155 (1987); **40**, 4977 (1989).
 - [13] G. Howat, T. Åberg, and O. Goscinsky, J. Phys. B **11**, 1575 (1978); G. Howat, *ibid.* **11**, 1589 (1978).
 - [14] K. R. Karim, M. H. Chen, and B. Crasemann, Phys. Rev. A **29**, 2605 (1984).
 - [15] J. Tulkki and T. Åberg, J. Phys. B **18**, L489 (1985).
 - [16] M. O. Krause, J. Phys. Chem. Ref. Data **8**, 307 (1979).
 - [17] T. Åberg and G. Howat, in *Handbuch der Physik*, edited by W. Mehlhorn (Springer, Berlin, 1982), Vol. 31, p. 469.
 - [18] K. R. Karim and B. Crasemann, Phys. Rev. A **31**, 709 (1985).
 - [19] I. P. Grant, B. J. McKenzie, P. H. Norrington, M. F. Mayers, and N. C. Pyper, Comp. Phys. Commun. **21**, 207 (1980); B. J. McKenzie, I. P. Grant, and P. H. Norrington, *ibid.* **21**, 233 (1980).
 - [20] U. Fano, Phys. Rev. **124**, 1866 (1961).
 - [21] M. H. Chen, B. Crasemann, and H. Mark, Phys. Rev. A **24**, 1158 (1981).
 - [22] M. H. Chen, B. Crasemann, N. Mårtensson, and B. Johansson, Phys. Rev. A **31**, 556 (1985).
 - [23] A. Wentzel, Z. Phys. **43**, 524 (1927).
 - [24] I. P. Grant, Meth. Comp. Chem. **2**, 1 (1988).
 - [25] P. O. Löwdin, Phys. Rev. **97**, 1474 (1955).
 - [26] S. Fritzsche, G. Zschornack, G. Musiol, and G. Soff, Phys. Rev. A **44**, 388 (1991).
 - [27] J. H. Scofield, At. Data Nucl. Data Tables **14**, 121 (1974).